Development of a multi-layer microreactor: Application to the selective hydrogenation of 1-butyne

G. García Colli[a,b], J.A. Alves[a,b,*], O.M. Martínez[a,b], G.F. Barreto[a,b]

[a] Departamento de Ingeniería Química, Facultad de Ingeniería (UNLP) La Plata, Argentina
[b] Centro de Investigación y Desarrollo en Ciencias Aplicadas "Dr. J. J. Ronco" (CINDECA) CCT-La Plata-CONICET-UNLP, Argentina

A B S T R A C T

A multi-layer microreactor (MR) was especially developed to assess the effects of the intensification of liquid-phase selective hydrogenation of 1-butyne (BY). The behavior of the system is described and the results of the regression of experimental data are reported. Various MR configurations, differentiated by the number of catalyst layers were constructed. A commercial Pd/Al$_2$O$_3$ catalyst, crushed and sieved to 37–44 μm particle size, has been tested. The reaction was carried out in liquid phase, at three levels of temperature (35, 44 and 60 °C), and covering a range of hydrogen partial pressure of 1.2–5 bar. The kinetic expression used to analyze the experimental data was based on an elementary step mechanism. Fitting of the kinetic parameters allowed to reproduce the experimental results within an average deviation of 3.7%. The results presented in this study are compared to experimental data obtained previously on the same commercial catalyst, but using the original 2.3 mm spherical pellets packed in a conventional fixed bed reactor (FBR). It is concluded from such a comparison that the measurements carried out in the MR are free from diffusion limitations and that the evaluation of such effects in the FBR was satisfactorily performed.

© 2016 Elsevier B.V. All rights reserved.

1. Introduction

The purification of C4-rich cuts, mainly from Fluidized Catalytic Cracking, for the industrial production of high purity 1-butene (1BE) is carried out by selective hydrogenation of 1,3-butadiene (BD) and acetylenic compounds, typically 1-butyne (BY), on Al$_2$O$_3$ supported Pd catalysts [1]. Commercial catalysts are of egg-shell type. High purity 1BE is used in the production of polybutenes and as co-monomer for low-density polyethylene. Current technologies employ catalytic fixed beds with cocurrent flow – either down or upflow – of the liquid hydrocarbon mixture and hydrogen [1]. Operating temperatures are between 20 and 60 °C; total pressure within the range of 8–20 bar to operate with hydrocarbons in liquid-phase.

BD and BY concentrations in the raw stream usually reach around 1 mol%. The target of selective hydrogenation for 1BE purification is to reduce the amount of impurities to about 20 ppm, with minimal loss of 1BE.

We previously verified [2–4] that reactions proceed under strong diffusion limitations inside the active shell of the catalyst particles, causing significant losses of the substance to be purified, 1BE. Although the use of slurry reactors with sufficiently small catalyst pellets can reduce diffusional limitations, the industrial application is inappropriate due to costly filtration steps that would be necessary.

Although many studies on selective hydrogenation on Pd have been reported in the literature, most of them focus on qualitative aspects such as the effect of metallic particle size, presence and type of promoters, identification of product distribution, reaction mechanisms and catalyst deactivation, as caused by oligomer formation on the catalytic surfaces [5,6].

As discussed by Alves et al. [4], the development of kinetic expressions and parameter estimation has been scarcely undertaken, and in most instances the range of experimental conditions has not been wide enough for the purpose of simulating or sizing industrial reactors

We carried out a complete kinetic characterization of the reactions on a commercial egg-shell catalyst [3,4,7,8]. Specifically for the hydrogenation reaction of BY, Alves et al. [8] presented a kinetic model and the estimation of the corresponding parameters, covering a temperature range of 27–62 °C. Experiments performed

Table 1
Catalyst features [23].

Shape	Sphere	Specific surface area of Pd	$0.55\,\mathrm{m^2/g}$
Type	Egg-shell	Metal particle size	$3.6\,\mathrm{nm}$
Diameter	$2.3\,\mathrm{mm}$	Dispersion	27%
Bulk density	$1150\,\mathrm{kg/m^3}$	Tortuosity factor	1.5 ± 0.6
Active shell volumetric fracction	0.49	Mean pore radius	$37 \pm 6\,\mathrm{nm}$
Pd load	0.2% w/w	Active shell thickness	$0.23\,\mathrm{mm}$
Specific surface area BET	$70 \pm 20\,\mathrm{m^2/g}$	Porosity	0.4

until almost 100% BY conversion (i.e., when BY in the mixture reaches around 20 ppm) allowed identifying the (−1) and zeroth-order regimes that arise in the course of BY consumption.

For the analysis of any catalytic reactor it is desirable to have an experimental tool to provide reliable kinetic information in order to determine intrinsic kinetic parameters without the potential masking effect caused by resistance to heat and mass transport. In this sense, the microreactors are an interesting option to study this reactive system in the laboratory. These devices feature fluid channels with lengths in the millimeter-to-centimeter range and cross-sectional dimensions in the sub-micrometer to sub-millimeter range [9–11]. Due to these small dimensions, microreactors have high surface/volume ratios (in the order $10^4\,\mathrm{m^2/m^3}$) that result in improved heat and mass transfer characteristics, critical for carrying out chemical reactions efficiently [12–14].

The integration of a solid catalytic phase (heterogeneous catalyst) in microreactors is a challenging task. Conventionally, it is achieved by two methods:

a) By using a micro packed-bed of powdered catalyst [15–17], or
b) By using a thin layer of catalyst coating on the inner walls of microchannels [18–20].

These two alternatives are not exempt from drawbacks, since a powdered catalyst micro packed-bed might result in high pressure drops along the length of the reaction-channel, whereas a thin catalyst coating usually fails to utilize the entire volume of the reactor channel effectively.

In this work, the behavior of an experimental microreactor (MR) developed to study the intensification of selective hydrogenation of BY on milled samples of a commercial Pd/Al$_2$O$_3$ catalyst, and regression of experimental data are described. These results are contrasted with those obtained in tests performed in a conventional fixed bed reactor (FBR), in order to verify their consistency and highlight the difference between the two systems regarding the difficulty to obtain the correct experimental data.

2. Experimental

2.1. Materials

The tests were performed on a commercial catalyst Pd loading of 0.2 wt%. The results of the characterization of the catalyst are shown in Table 1.

The commercial catalyst was crushed and sieved to 37–44 μm in the experiments performed with the MR. Previous measurements in the FBR were conducted with the catalyst in its original form, spherical pellets of 2.3 mm diameter with an active shell 0.23 mm thick (egg-shell configuration).

H$_2$ (99.999%) and N$_2$ (99.999%) were provided by Linde-AGA. BY (99.999%) and n-Propane (99.999%) were provided by Alphagas. n-hexane (95% HPLC, provided by UVE) served as inert solvent. For assembling the reactor, commercial nylon membranes were used (0.1 mm thick, with a pore diameter of 0.8 μm) (provided by OSMONICS).

Before each run, the compounds fed to the experimental system were purified as described in the next paragraph. The main objective of the purification procedure was to minimize the presence of moisture in the reaction mixture, since it severely impaired catalyst activity [2]. To this purpose, BY, propane and n-hexane were fed after flowing through individual beds of 4A molecular sieve (UOP) and a guard-bed loaded with the same catalyst as used in the experiments. H$_2$ and N$_2$ were purified from water and oxygen by passing the streams through a guard-bed followed by a bed of 4A molecular sieve and an oxygen trap (Oxy-Trap, Alltech).

2.2. Experimental set up

Batch experiments regarding the unsaturated hydrocarbons were performed using the experimental setup whose scheme is shown in Fig. 1.

The 100 ml-stirred vessel (Autoclave Engineers EZE-Seal) was used for loading the initial hydrocarbon mixture, feeding H$_2$ continuously, and maintaining the liquid saturated with H$_2$ during the runs. The vessel was furnished with an impeller that allows the headspace gas to be dispersed into the stirred liquid. A control tower (Autoclave Engineers CT-100) allowed setting the agitation speed (up to 3000 rpm) and temperature control by means of an electrical heater that encloses the vessel. Gas and liquid samples were taken off by means of two valves connected to the vessel. The agitation speed in the stirred vessel was set at 2000 rpm. It was confirmed that at 2000 rpm the mass transport between the swarm of bubbles and the liquid is efficient enough to saturate the latter with hydrogen at reaction conditions. A magnetically driven gear micropump (Micropump 200) was used to recirculate (700 ml/min) the reaction mixture at high rate from the stirred vessel to the external reactor and back to the vessel.

Apart from the desired unsaturated hydrocarbons, n-hexane was used as an inert solvent to facilitate the manipulation of the samples analyzed chromatographically. Also, a certain amount of propane was used for independent control of hydrogen partial pressure (p$_{H2}$) and total pressure. The reactor, sketched in Fig. 1, represents the MR used in this study or the FBR previously used.
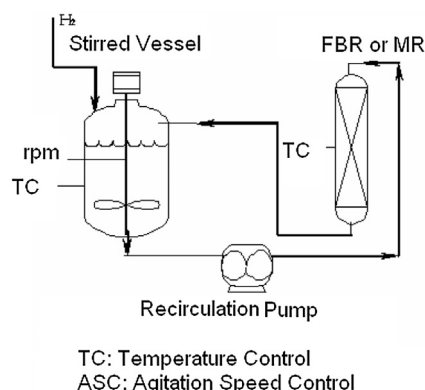

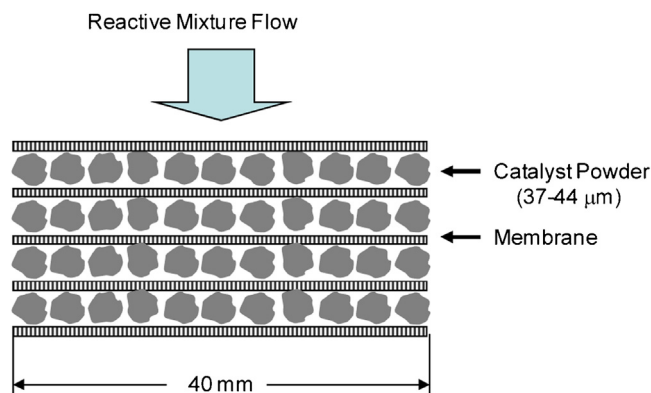Fig. 1. Scheme of experimental setup.

Fig. 2. Micro Reactor (MR): configuration with 4 layers.

2.3. Fixed bed reactor (FBR)

The external fixed-bed reactor consists of a 1/4 in. o.d. stainless steel tube surrounded by a jacket. The tube is filled with a sample of catalyst pellets in their original size. A thermocouple placed inside the tube allows reading the reactive mixture temperature. Water from a thermostatic bath at the same temperature of the stirred vessel was recirculated inside the jacket.

Thus, the whole loop in Fig. 1 operated under a uniform temperature level which was maintained constant during each experimental run. Some other details concerning the experimental system and the FBR were described by Ardiaca et al. [2].

2.4. Micro-reactor (MR)

In the final configuration adopted for the MR, the catalyst powder is arranged in four layers with a thickness of about 50 μm, approximately equivalent to the size of a catalyst particle, and 4 cm diameter each, separated by nylon membrane discs (see Fig. 2).

Both the active shell and the non-impregnated portion of the catalyst pellets have the same support, i.e. α-Al$_2$O$_3$. As a result, there is no reason to expect non-homogeneus samples from the grinding process. This is backed by the very good reproducibility observed between tests performed with different samples of catalyst. A sintered bronze disc, 50 μm pore size, supports membranes and catalyst layers. The catalyst is loaded on nylon membrane discs by spreading catalyst powder with a spatula. After the first layer, membranes and catalyst layers are overlapped until the required catalyst mass is reached. The set of membranes and layers are wetted with solvent (n-hexane) with the objective of keeping the catalyst particles fixed during handling. The catalyst layers and nylon membranes are sealed by one viton O-ring to prevent any peripheral leakage of fluid during operation. This set of accessories is placed within a body formed by two suitably machined brass parts. Electric heating tape, controlled by a rheostat, maintains a constant temperature throughout the reactor.

The disposition of the catalyst in four layers allows a homogeneous spatial distribution; thus a uniform flow distribution is achieved through the catalyst; this is due to the pressure drop around the recirculation loop being controlled by the resistance of the membranes. In Section 4.1 the reason for the adoption of four layers of catalyst is discussed

A recirculating flow rate of 700 ml/min is high enough to produce low conversions per pass of hydrogen and unsaturated hydrocarbons (<3%). This allows considering a uniform reaction rate in the catalyst layers (assuming uniform liquid flow distribution in the cross section).

2.5. Experimental procedure

Catalyst samples were reduced in situ in the reactor in Fig. 1. Following the manufacturer's indications, an H$_2$/N$_2$ (1:1) stream (total flow 200 ml/min) was used as reducing agent for 8 hs at 100 °C. Then the n-hexane was introduced into the stirred vessel, the desired amounts of unsaturated hydrocarbons were dissolved and, if necessary, n-propane, was used when working pressure was too low to extract the liquid samples. Finally the hydrogen feed was connected, thereby fixing the operating pressure of the system. The hydrocarbons present in the reaction mixture were n-propane, n-hexane and the C4 hydrocarbons involved in the reaction system (i.e. BY, 1BE, cis and trans 2-butene (cBE, tBE) and n-butane (BA)). Liquid samples were taken frequently during the course of the reaction and were subjected to gas chromatography analyis using a FID detector (Shimadzu GC-8A) furnished and with a 7 feet long, 1/800 diameter column packed with 0.19% of picric acid on 80–100 Graphpac mesh (Alltech). The steadiness of hydrogen partial pressure along each experimental run was tested by injecting samples of the vapor-phase to a conductivity cell.

3. Overall reaction network and kinetic model

The overall set of reactions that occur from the hydrogenation of BY can be scketched as in Fig. 3. The primary product, 1BE, can be catalytically isomerized to cBE or tBE, and also hydrogenated to BA. Such reactions should be avoided to prevent loss of 1BE. This is possible because BY is strongly and preferentially adsorbed on active sites, so that they are not available for the 1BE adsorption, even at very low BY concentrations.

In this work only the regression of experimental data corresponding to the BY hydrogenation reaction will be presented.

The kinetic expression derived from the proposal of Boitiaux et al. [22] and Hub and Touroude [23], which leads to the mechanism described in Table 2, is able to represent a negative order with respect to BY which was observed experimentally. This mechanism postulates that a BY molecule adsorbed on one metal site, π-adsorbed intermediate, represented by BY⊗ in the elementary step (e2), is in equilibrium with a more stable complex that consists of two molecules of BY adsorbed on one metal site, σ-diadsorbed intermediate, (BY)$_2$⊗ in the elementary step (e3). The elementary step (e4) shows that only the π-adsorbed intermediate is active for BY hydrogenation. The complex (BY)$_2$⊗ is so stable that it remains inactive, but its presence is required to obtain a negative order with respect to BY. It is assumed that elementary step (e5), is the kinetically controlling step. We
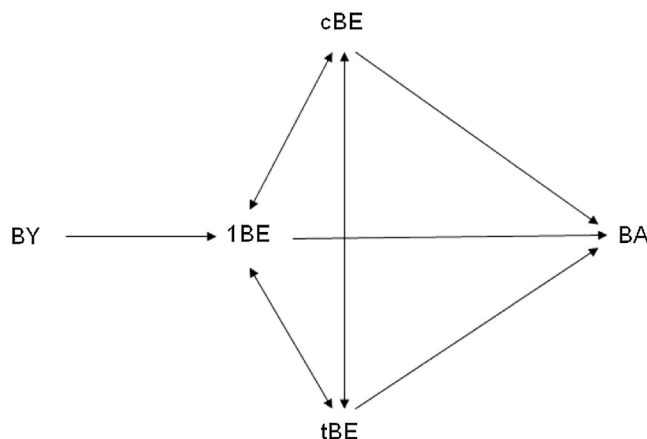

Fig. 3. Scheme of global reactions.

Table 2
Catalytic mechanism for the hydrogenation of BY.

(e1) $H_2 + 2* \overset{K_{H_2}}{\rightleftarrows} 2(H*)$	(e4) $BY \otimes + H* \rightleftarrows C_4H_7 \otimes +*$
(e2) $BY + \otimes \overset{K_{BY}}{\rightleftarrows} BY\otimes$	(e5) $C_4H_7 \otimes + H* \overset{k}{\rightarrow} 1-BE\otimes$
(e3) $BY + BY\otimes \overset{K_\eta}{\rightleftarrows} (BY)_2\otimes$	(e6) $1-BE + \otimes \overset{K_{1BE}}{\rightleftarrows} 1-BE\otimes$

also assumed that the fraction of active sites "$\otimes$" covered by the semihydrogenated reaction intermediate $(C_4H_7)\otimes$ is negligible.

It was further assumed that there is no competition between BY and H_2 for the same active sites. Furthermore, it was assumed that the hydrogen adatoms are originated from the dissociative adsorption of hydrogen molecules.

The assumptions made were validated by Alves et al. [4] for the hydrogenation of 1,3 butadiene and by Bressa et al. [21] for the hydrogenation and hydroisomerization of 1-butene. Under these statements, the following kinetic expression was obtained:

$$r = \frac{k\,K_{BY}\,x_{BY}}{1 + K_{BY}x_{BY}(1 + K_\eta x_{BY}) + K_{1BE}x_{1BE}} F(x_{H_2}) \qquad (1)$$

with

$$F(x_{H_2}) = \frac{x_{H_2}}{(1 + \gamma\sqrt{K_{H_2}x_{H_2}})(1 + \sqrt{K_{H_2}x_{H_2}})} \qquad (2)$$

where x_j are the mole fractions of j, K_{BY} is the adsorption constant of BY (step e2), K_η is the adsorption constant of complex $(BY)_2\otimes$ (step e3), k is the kinetic coefficient, K_{H_2} is the adsorption constant of H_2 (step e1), K_{1BE} is the adsorption constant of 1BE (step e6) and γ is an independent parameter related to the specific coefficients of the elementary steps e4 and e5. The two surface species of BY are strongly adsorbed, such that $1 + K_{1BE}\,x_{1BE} << K_{BY}\,x_{BY}\,(1 + K_\eta\,x_{BY})$. Therefore, except for very low values of x_{BY}, Eq. (1) can be re-expressed as:

$$r = \frac{k}{1 + K_\eta x_{BY}} F(x_{H_2}) \qquad (3)$$

4. Results and discussion

4.1. Design of MR

The typical evolution of the hydrocarbon molar fractions for a test conducted in the MR, with a configuration of four catalyst layers, is presented in Fig. 4. The data corresponding to cBE and tBE are not plotted to facilitate interpretation. Symbols represent experimental data. As shown in Fig. 4 BY hydrogenation proceeds with negative reaction order until it almost disappears.
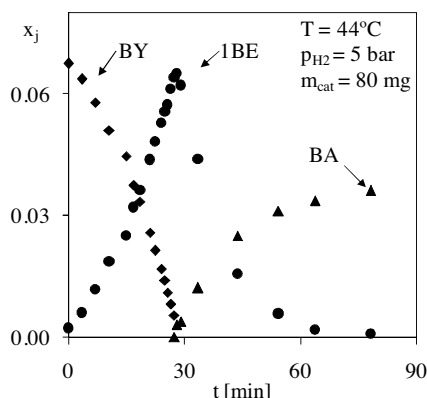
Also, the 1BE produced begins to react only when the BY is nearly extinct. This confirms, on the one hand, the high intrinsic selectivity of the catalyst. Additionally, it indicates that the BY concentration in the fluid bulk is very similar to that in contact with the active sites of the catalyst, as a result of the absence of transport effects both outside and inside of the catalyst particles. In this situation there are no free active sites for the 1BE adsorb and react with H_2.

Selectivity $S = (x_{1BE} - x_{1BE0})/(x_{BY0} - x_{BY})$ was a decisive variable for setting the final configuration of MR. Values of S for the same volume of catalyst sample, distributed in different number of catalyst layers, as a function of the residual ppm of BY (solid lines are trend lines) are shown in Fig. 5. It can be seen that for a single layer S decreases permanently up to only 20% at the time BY is totally consumed.

This behavior can be explained considering the difficulty of controlling the uniformity of catalyst layer thickness (about 200 μm, for a single layer). It follows that the catalytic powder may accumulate in certain areas, generating insufficient irrigation, and consequent reduction in BY concentration. The catalyst active centers would then be exposed to 1BE adsorption and subsequent reaction. The catalyst sample distribution in two layers partially avoids the above mentioned effect, reaching S = 50% at the time of termination of BY, while the division into four or more layers leads to achieve high values of selectivity (over 90%) until disappearance of BY, indicating that the particles in each layer are isolated enough to virtually eliminate localized accumulation. For practical reasons, therefore, the configuration with four catalyst layers was adopted, corresponding to a catalyst layer thickness ($\approx$50 μm) similar to the diameter of a single powder particle.

The MR, applied to other reactive systems, will require a number of catalyst layers and reactor diameter that ensure, as explained in the previous paragraph, a catalyst layer of uniform thickness and with the catalyst particles virtually isolated. The overall catalyst mass used in the experiments will depend on the reaction rate and the desired duration of the experimental tests.

The simple construction of the MR presented here, renders its use for kinetic tests advantageous over other devices of sophisticated construction, as proposed by Ajmera et al. [24]. Furthermore, although the slurry reactor may be applied to the study of liquid phase reactions, it requires additional operations when it is desired to recover the catalyst sample and it can also introduce operating difficulties such as those indicated by Ardiaca et al. [2] for a system like the one studied here.

4.2. Regression of the experimental data obtained from MR

A set of seven experiments was performed at 44 °C to adjust the parameters of the kinetic model expressed by Eq. (3). Three p_{H2} levels, 1.2, 3.2 and 5 bar were used, and in each case the tests with
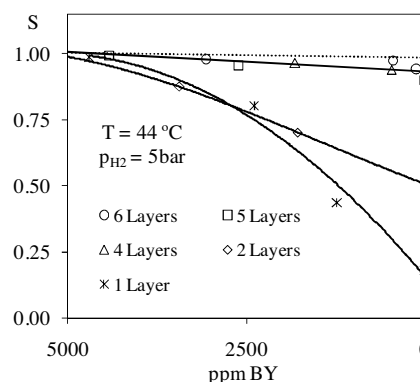

Fig. 4. Evolution of the composition in the MR.

Fig. 5. Selectivity as a function of the residual ppm of BY to configurations 1, 2, 4, 5 and 6 catalyst layers.

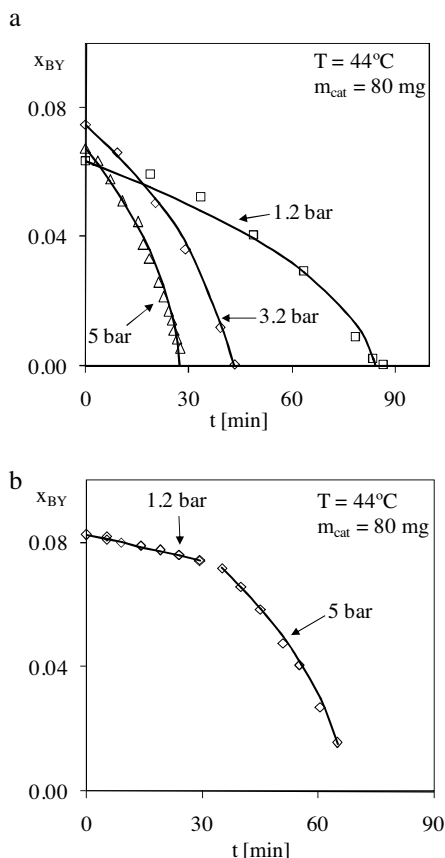Fig. 7. Evolution of the composition in the FBR.

Fig. 6. a. Measured (symbols) and predicted (solid lines) BY mole fraction at different values of p_{H2}. The results were obtained in the MR using three different catalyst samples. b. Measured (symbols) and predicted (solid lines) BY mole fraction. The experimental data were obtained in the MR by changing p_{H2} in the course of the experimental run.

different samples of catalyst were repeated, showing excellent reproducibility. The seventh test was performed by changing the p_{H2} during the run on two levels, 1.2 and 5 bar. In each test the composition of a set of samples was analyzed at different reaction times, as illustrated in Fig. 4. The conservation equation corresponding to BY during each experimental run is:

$$\frac{d(N_T x_{BY})}{dt} = - m_{cat} v_{act} r \tag{4}$$

where N_T is the total mole number in the system, m_{cat} is the mass of the catalyst sample and v_{act} is the active shell volume per unit mass of catalyst ($4.3 \times 10^{-4}\,\mathrm{m^3_{act}/kg_{cat}}$).

The amount of hydrocarbons in the vapor phase was neglected, as it represents a fraction less than 2%. However, the total volume of liquid phase extracted during sampling is approximately 10–20% of the initial batch, so N_T was corrected after each extraction. The distribution of the species in the liquid and vapor phases were evaluated with the Redlich–Kwong–Soave equation of state modified by Graboski and Daubert [25].

Given trial values for kinetic parameters, the integration of Eq. (4) allows to obtain predicted values of x_{BY}. Based on this basic procedure, the regression of the experimental data for estimating the optimal kinetic parameters was performed with the GREGPAK subroutines package [26]. Further details on data analysis have been reported in our earlier communications [3,4].

The $F(x_{H2})$ factor according to Eq. (2) involves the determination of two parameters (γ and K_{H2}). A preliminary regression
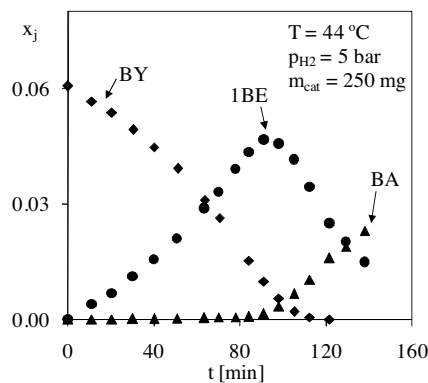
indicated that the experimental range $1 < p_{H2} < 5$ bar was not wide enough to discriminate both parameters, so Eq. (2) was simplified in the form $F(x_{H2}) = x_{H2}/\left(1 + \delta x_{H_2}^{0.5}\right)$ considering δ as an empirically adjustable parameter. Then, the expression finally tested was:

$$r = \frac{k}{1 + K_\eta x_{BY}} \frac{x_{H_2}}{1 + \delta x_{H_2}^{0.5}} \tag{5}$$

Eq. (5) predicts the experimental data with an average deviation of 3.7%, resulting $k = (3.00 \pm 0.68)\ 10^6\,\mathrm{mol\,s^{-1}\,m^{-3}_{act}}$, $K_\eta = (175 \pm 34)$ and $\delta = (21.9 \pm 5.9)$. Confidence intervals correspond to a 95% of the normal distribution.

The kinetic model predictions (solid lines) and experimental data (symbols) are presented in Fig. 6a and b. The experimental data in Fig. 6a were obtained from three different samples of catalyst tested at different values of p_{H2}. Instead, the data in Fig. 6b corresponds to a single test, in which p_{H2} was changed in the course of the run.

With these results, the behavior of the kinetic model can be considered highly satisfactory. It is emphasized that the coefficient k is expressed per unit volume of the original catalyst active shell. The results at other temperatures are discussed in Section 4.4.

4.3. Comparison of the performance of whole (FBR) and milled (MR) catalyst particles

In Fig. 7, the experimental variation of hydrocarbons mole fraction as a function of time, is presented for a test performed in the FBR.

The operating conditions were the same as those in the test conducted with the MR of Fig. 4, i.e., $p_{H2} = 5$ bar and temperature of 44C.

As in the test performed with the MR, a negative effective reaction-order can be noticed for the hydrogenation of BY. However, when comparing the performance of both reactors, 1BE consumption is noticeable at significantly higher values of x_{BY} in the FBR, as can be shown more clearly in Fig. 8, where the selectivity S is presented for both reactors as a function of the BY ppm at different values of p_{H2} (solid lines are trend lines). Therefore, to obtain the almost complete disappearance of BY, as required in the industrial process, the selectivity achieved in the MR is about 90%, independently of the value of p_{H2}, while the selectivity in the FBR reaches values around 40% and 60% for $p_{H2} = 5$ bar and $p_{H2} = 3$ bar, respectively. This means that the FBR has a significantly lower selectivity which also deteriorates sharply with increasing p_{H2} [2–4,7]. This difference is due to the strong diffusional resistance inside the active shell of commercial catalyst
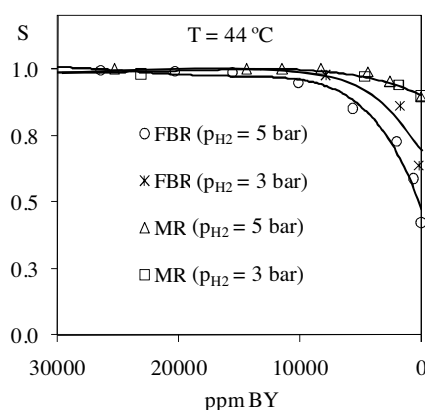
Fig. 8. Comparison of the selectivity between the MR and FBR.

Another alternative which allows to check the quality of the information obtained in the MR and the consistency thereof with previous results, was provided by two tests in the reactor at 35 and 60 °C. In the kinetic expression (3), the effect of temperature is relevant because of its impact on the rate constant k and the adsorption constant K_η. Given that the number of tests and temperature levels are insufficient to fit the dependency of both parameters with temperature, it is preferred to compare the results of such tests with the predictions obtained using the values of activation energy $E_a(k)$ and ΔH heat of adsorption (for K_η) estimated from tests on the FBR. Alves et al. [8] expresed:

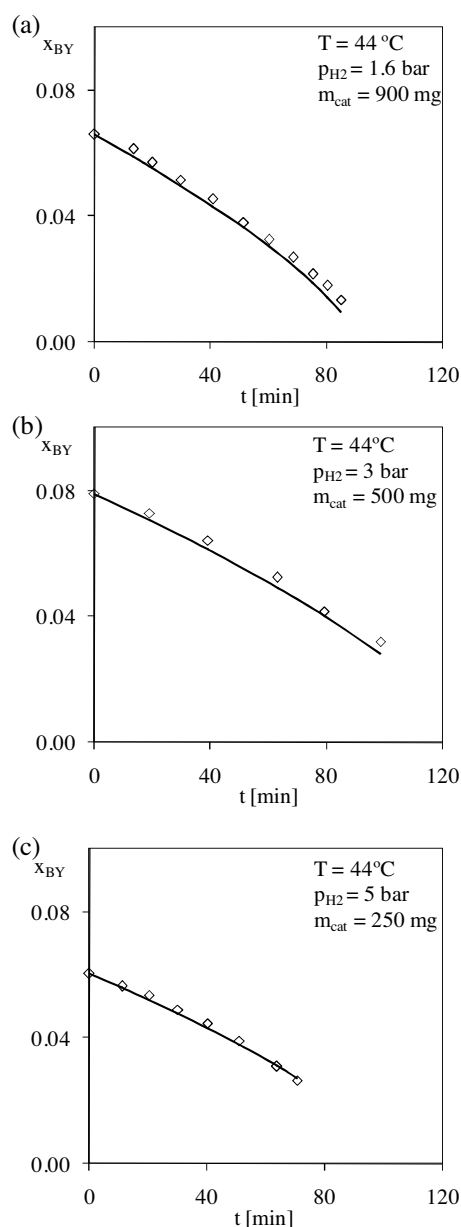$$k(T) = k(T_{ref})\exp\left[-\frac{E_a}{R}\left(\frac{1}{T} - \frac{1}{T_{ref}}\right)\right] \qquad (6)$$

in the FBR. Consequently, when BY becomes the limiting reagent, the excess of H_2 and the availability of active sites allow 1BE consumption. Instead, in the MR, which uses milled catalyst, the Weisz modulus [27] proved that there is no mass transfer resistance in the porous medium.

To quantify the decrease in activity produced by diffusional resistance, the reference will be the reaction time in which the BY is completely consumed. In the MR, using 80 mg of catalyst, 30 min are required (see Fig. 4), while in the FBR using 250 mg of catalyst, time is 120 min (see Fig. 7). This implies an overall consumption rate of BY 12.5 times higher in the MR for the same operating conditions.

4.4. Checking of measurements consistency between tests performed in the MR and the FBR

In a previous study [8] using the FBR, the quantification of the` diffusion resistance in the analysis of the results allowed to estimate the rate constant k and the constant K_η.

However, these values cannot be directly compared to those reported in Section 4.2 because of two main reasons. First, $F(x_{H2}) \equiv x_{H2}$ has been used in [8], while the expression $F(x_{H2}) = x_{H2}/\left(1 + \delta x_{H2}^{0.5}\right)$ used presently in Eq. (5) weights differently the effect of p_{H2}, a fact that is reflected in the estimates of k and K_η. On the other hand, the active shell thickness (0.23 mm) was mistakenly used in [8] as the characteristic length of the catalyst pellet, whereas the correct value should be the ratio between the active shell volume and the outer surface area of the catalyst pellet (0.19 mm). Therefore, to assess the consistency between the experiments performed in both types of reactors, FBR and MR, it has been found better to compare the experimental data obtained at 44 °C in the FBR with predicted values arisen by coupling Eq. (5), and the parameter values reported in Section 4.2, with the model and transport parameters proposed by Alves et al. [8]. The comparison of the experimental (symbols) and predicted (solid lines) values performed for three experiments at different p_{H2} is shown in Fig. 9. The average deviation of only 4.2% confirms that the values of the rate constant k and the constant K_η estimated in the MR can successfully predict the experimental data obtained in the FBR at 44 °C. The simulation was performed until hydrogen was no longer the limiting reagent and, as explained, H_2 begins to be consumed by 1BE. Consequently x_{H2} profile in the active shell will be affected by this consumption. The evaluation of this effect would require the kinetic characterization of 1BE reactions in the MR, a topic that is outside the scope of this work.

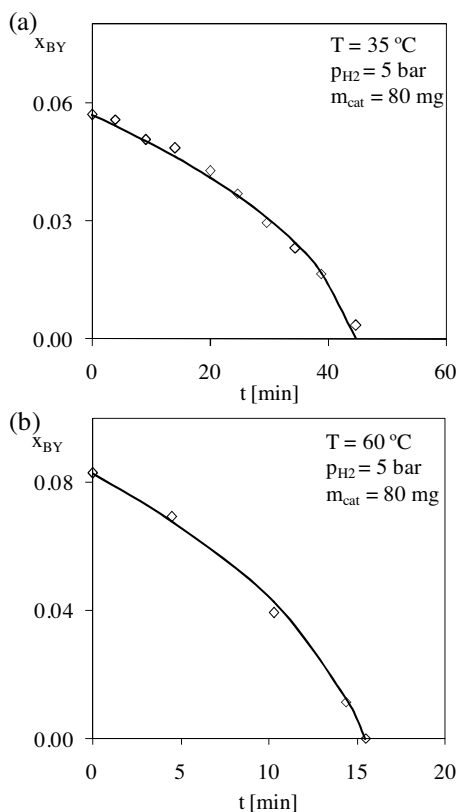**Fig. 9.** Simulation (solid lines) of the tests performed in the FBR (symbols) at different p_{H2}.

Fig. 10. Simulation (solid lines) of the tests performed in the MR (symbols) at different temperatures.

$$K_\eta(T) = K_\eta(T_{ref}) \exp\left[-\frac{\Delta H}{R}\left(\frac{1}{T} - \frac{1}{T_{ref}}\right)\right] \tag{7}$$

where $T_{ref} = (273 + 44)$ °K. The estimated values of the kinetic parameters were $E_a = (32 \pm 3)$ 10^3 J mol^{-1} y $\Delta H = (-34 \pm 3)$ 10^3 J mol^{-1} [8]. The experimental results (symbols) and the estimates predicted (solid lines) using Eq. (5) with the values of $k(T_{ref})$, $K_\eta(T_{ref})$ and δ reported in Section 4.2 and E_a and ΔH values obtained by Alves et al. [8] are shown in Fig. 10.

The average deviation between predictions and measurements is 3.2%, a value which confirms that the estimated values of the activation energy and enthalpy of adsorption from the FBR are able to adequately represent the experimental data obtained in the MR at 35 and 60 °C. The analysis conducted in this section shows that the results of the MR correspond to catalyst intrinsic kinetics and, simultaneously, checks the validity of the model and the transport parameter values previously used by the authors to regress the experimental data gathered from the FBR [3,4,7,8,28].

5. Conclusions

In this paper, a new micro-reactor (MR) consisting of four thin layers of catalyst powder separated by commercial nylon porous membranes, was presented in order to studying the selective catalytic hydrogenation of BY. A commercial egg-shell catalyst was ground to a particle size between 37 and 44 μm. During the design stage of the MR different configurations with one, two, four, five and six catalyst layers were tested, finally four layers were adopted. Fitting a kinetic expression for hydrogenating BY based on a mechanism of elementary steps, allowed faithfully reproduce the experimental results. The results achieved in the MR were

compared with those previously obtained in the FBR with the same catalyst, but using catalyst pellets in their original size (2.3 mm in diameter) which exhibited strong diffusional effects. The MR showed a significant increase in catalytic activity (12.5 times greater) and selectivity. The simulation conducted on different groups of tests proved that MR experimental data are consistent with the tests already performed in the FBR. Everything indicates that the MR is an appropriate tool for the kinetic study of catalysts. This provides us with a reliable description of the intrinsic reaction kinetics, essential for the design of industrial scale chemical reactors.

References

[1] M.L. Derrien, Selective hydrogenation applied to the refining of petrochemical raw materials produced by steam cracking, Stud. Surf. Sci. Catal. 27 (1986) 613–666.
[2] N.O. Ardiaca, S.P. Bressa, J.A. Alves, O.M. Martinez, G.F. Barreto, Experimental procedure for kinetic studies on egg-shell catalysts: the case of liquid-phase hydrogenation of 1,3-butadiene and n-butenes on commercial Pd catalysts, Catal. Today 64/3–4 (2001) 205–215.
[3] J.A. Alves, S.P. Bressa, O.M. Martínez, G.F. Barreto, Study of the selective catalytic hydrogenation of 1,3-butadiene in a mixture of n-butenes, J. Ind. Eng. Chem. 18 (2012) 1353–1365.
[4] J.A. Alves, S.P. Bressa, O.M. Martínez, G.F. Barreto, Kinetic evaluation of the set of reactions in the selective hydrogenation of 1-butyne and 1,3-butadiene in presence of n-butenes, Ind. Eng. Chem. Res. 52 (2013) 5849–5861.
[5] J. Silvestre-Albero, G. Rupprechter, H.-J. Freund, Atmospheric pressure studies of selective 1,3-butadiene hydrogenation on well-defined Pd/Al$_2$O$_3$/NiAl(110) model catalysts, J. Catal. 240 (2006) 58–65.
[6] J. Gaube, H.-F. Klein, Kinetics and mechanism of butene isomerization/hydrogenation and of 1,3-butadiene hydrogenation on palladium, Appl. Catal. A Gen. 470 (2014) 361–368.
[7] J.A. Alves, Cinética de la hidrogenación catalítica selectiva de 1-butino y 1,3-butadieno en presencia de n-butenos Tesis Doctoral, Universidad Nacional de La Plata (2009).
[8] J.A. Alves, S.P. Bressa, O.M. Martínez, G.F. Barreto, Kinetic study of the liquid-phase selective hydrogenation of 1-butyne in presence of 1-butene over a commercial palladium-based catalyst, Chem. Eng. Res. Des. 89 (2011) 384–397.
[9] S.K. Ajmera, C. Delattre, M.A. Schmidt, K.F. Jensen, Microfabricated differential reactor for heterogeneous gas phase catalyst testing, J. Catal. 209 (July (2)) (2002) 401–412.
[10] W. Ehrfeld, V. Hessel, H. Lowe, Microreactors—New Technology for Modern Chemistry, first ed., Wiley-VCH, Weinheim, 2000.
[11] G. Kolb, V. Hessel, Micro-structured reactors for gas phase reactions, Chem. Eng. J. 98 (2004) 1–38.
[12] D. Gobby, P. Angeli, A. Gavriilidis, Mixing characteristics of T-type microfluidic mixers, J. Micromech. Microeng. 11 (March (2)) (2001) 126–132.
[13] S. Hardt, F. Schönfeld, Laminar mixing in different interdigital micromixers. II. Numerical simulations, AIChE 49 (March (3)) (2003) 578–584.
[14] E.R. Delsman, M.H.J.M. Croon de, G.J. Kramer, P.D. Cobden, C. Hofmann, V. Cominos, J.C. Schouten, Experiments and modeling of an integrated preferential oxidation-heat exchanger microdevice, Chem. Eng. J. 101 (August (1–3)) (2004) 123–131.
[15] S.K. Ajmera, C. Delattre, M.A. Schmidt, K.F. Jensen, Microreactors for measuring catalyst activity and determining reaction kinetics, Stud. Surf. Sci. Catal. 145 (2003) 97–102.
[16] C.D. Baertsch, M.A. Schmidt, K.F. Jensen, Catalyst surface characterization in microfabricated reactors using pulse chemisorption, Chem. Commun. 22 (2004) 2610–2611.
[17] K. Shah, R.S. Besser, Development of an integrated silicon micro methanol steam reformer to understand thermal management issues in micro fuel processor, AIChE Annu. Meet., Conf. Proc., Cincinnati, OH, United States, Oct. 30–Nov. 4, 2005 36b/31–36b/38.
[18] K. Haas-Santo, O. Gorke, P. Pfeifer, K. Schubert, Catalyst coatings for microstructure reactors, Chimia 56 (2002) 605–610.
[19] K. Haas-Santo, M. Fichtner, K. Schubert, Preparation of microstructure compatible porous supports by sol-gel synthesis for catalyst coatings, Appl. Catal. A 220 (2001) 79–92.
[20] V. Meille, Review on methods to deposit catalysts on structured surfaces, Appl. Catal. A 315 (2006) 1–17.

[21] S.P. Bressa, O.M. Martínez, G.F. y Barreto, Kinetic Study of the hydrogenation and hydroisomerization of the n-butenes on a commercial palladium/alumina catalyst, Ind. Eng. Chem. Res. 42 (2003) 2081–2092.

[22] J.P. Boitiaux, J. Cosyns, E. Robert, Liquid phase hydrogenation of unsaturated hydrocarbons on palladium, platinum and rhodium catalysts. part i: kinetic study of 1-butene, 1 3-butadiene and 1- butyne hydrogenation on platinum, Appl. Catal. 32 (1987) 145–168.

[23] S. Hub, R. Touroude, Mechanism of catalytic hydrogenation of but 1 ene on palladium, J. Catal. 1146 (1988) 411–421.

[24] S.K. Ajmera, C. Delattre, M.A. Schmidt, K.F. Jensen, Microfabricated cross-flow chemical reactor for catalysts testing, Sens. Actuators B 82 (2002) 297–306.

[25] M. Graboski, T. Daubert, A modified Soave equation of state for phase equilibrium calculations. Systems containing hydrogen, Ind. Eng. Chem. Process Des. Dev. 18 (2) (1979) 300–306.

[26] W.E. Stewart, M. Caracotsios, J.P. Sørensen, Parameter estimation from multiresponse data, AIChE J. 38 (1992) 641–650.

[27] P.B. Weisz, J.S. Hicks, The behaviour of porous catalyst particles in view of internal mass and heat diffusion effects, Chem. Eng. Sci. 17 (1962) 265–275.

[28] J.A. Alves, S.P. Bressa, O.M. Martínez, G.F. Barreto, Kinetic study of the liquid-Phase hydrogenation of 1- butyne over a commercial Palladium/Alumina catalyst, Chem. Eng. J. 125 (2007) 131–138.